**Impact of PEGylation on the degradation and pore organization in Mesoporous Silica Nanoparticles: a study of the inner mesoporous structure in physiologically relevant ionic conditions**

María de los Ángeles Ramírez[1,2#], Elisa Bindini[1#], Paolo Moretti[3], Galo J. A. A. Soler Illia[2*], Heinz Amenitsch[4], Patrizia Andreozzi[1,5*], Maria Grazia Ortore[3*], Sergio E. Moya[1*]

[1]Soft Matter Nanotechnology Group, CIC biomaGUNE, Basque Research and Technology Alliance (BRTA), Paseo Miramón 182, 20014 San Sebastián, Guipúzcoa, Spain

[2] Instituto de Nanosistemas, UNSAM, CONICET, Avenida 25 de Mayo 1021, 1650 San Martín, Buenos Aires, Argentina

[3] Department of Life and Environmental Science, Marche Polytechnic University, via Brecce bianche, I-60131, Ancona, Italy.

[4] Institute of Inorganic Chemistry, Graz University of Technology, Austria.

[5] Department of Chemistry 'Ugo Schiff', University of Florence, Via della Lastruccia 3/13, Sesto Fiorentino, Florence, 50019, Italy.

[#] Authors contributed equally

Corresponding authors:

Sergio E. Moya smoya@cicbiomagune.es

Maria Grazia Ortore m.g.ortore@univpm.it

Galo J. A. A. Soler-Illia gsoler-illia@unsam.edu.ar

Patrizia Andreozzi patrizia.andreozzi@unifi.it

Codice campo modificato

Codice campo modificato

Codice campo modificato

Total number of words:6513 Total number of figures:8

**Abstract**

The degradation of mesoporous silica nanoparticles (MSNs) in the biological milieu due to silica hydrolysis plays a fundamental role for the delivery of encapsulated drugs and therapeutics. However, little is known on the evolution of the pore arrangement in the MSNs in biologically relevant conditions. Small Angle X-ray scattering (SAXS) studies were performed on unmodified and PEGylated MSNs with a MCM-48 pore structure and average sizes of 140 nm, exposed to simulated body fluid solution (SBF) at pH 7.4 for different time intervals from 30 minutes to 24 hours. Experiments were performed with silica concentrations below, at and over 0.14 mg/mL, the saturation concentration of silica in water at physiological temperature. At silica concentrations of 1 mg/ml (oversaturation), unmodified MSNs show variation in interpore distances over 6 hours exposure to SBF, remaining constant thereafter. A decrease in radius of gyration is observed over the same time. Mesoporosity and radius of gyration of unmodified MSNs remain then unchanged up to 24 hours. PEGylated MSNs at 1 mg/mL concentration show a broader diffraction peak but no change in the position of the peak is observed following 24 hours exposure to SBF. PEGylated MSNs at 0.01 mg/mL show no diffraction peaks already after 30 min exposure to SBF, while at 0.14 mg/mL a small diffraction peak is present after 30 minutes exposure but disappears after 1 hour.

**Keywords:** mesoporous silica nanoparticles; degradation; simulated body fluid; SAXS; PEGylation.

## Introduction

The administration of drugs encapsulated in mesoporous silica nanoparticles (MSNs) is a promising alternative to transport poorly soluble or highly cytotoxic drugs, and to improve their pharmacokinetics and biodistribution profiles, protecting them from enzymatic degradation[1]. However, despite the advancement in biomedical research involving MSNs, their biodegradation *in vivo* is not fully understood, which is fundamental for evaluating their clinical efficacy and potential medical translation[2,3]. Mesoporous silica can be prone to dissolution in the biological milieu, depending on the pH and ionic characteristics of the medium, the area of exposed surface, the surface functionalization, and the degree of polymerization of the inorganic structure[4]. The adsorption of proteins from the biological medium[5,6] on the other hand can prevent MSN dissolution by covering the pore surface and limiting the area of the mesoporous material exposed to the aqueous media.

The degradation of MSNs has a major impact on release kinetics when MSNs are used as a vehicle for encapsulated drugs. In most cases, the release of the encapsulated drug is aimed at specific organs. Therefore, it is crucial to avoid an early degradation of the nanoparticles during circulation. On the other hand, a slow release of the drug can lead to a limited therapeutic action. For this reason, understanding and controlling the degradation of MSNs is essential for drug delivery when therapeutic applications are sought[7].

Surface modification with different polymers, particularly with polyethylene glycol (PEG), reduces the interaction of MSNs with proteins and the opsonization process, prolonging the circulation of nanoparticles *in vivo*. However, it has been demonstrated that PEG functionalization also alters the degradation kinetics of MSNs[8,9].

Although silica degradation in physiological media is well known, there are still very few reports aiming at in-depth analysis of the structural change of mesoporous materials under conditions similar to those prevailing in vivo[10,11].

It is known that the degradation of MSNs at physiological pH depends on the nanoparticle concentration, its specific surface area, morphology, pore size, degree of silica condensation and surface coating[7,8,12]. Because silica dissolution is driven by the difference in concentration with the medium under saturation of silicates, if the concentration of MSNs is below the saturation concentration of silica, the degradation will be faster and more efficient than at concentrations of silica over the saturation concentration, 0.14 mg/mL[13]. In fact, once saturation is reached, dissolved silica can nucleate and re-precipitate on the structure, in an equilibrium that might lead to nanoparticle aggregation[5].

In particular, recent works have suggested that the pore structure plays a relevant role in the dissolution, not only due to the high surface area, but by enhancing the diffusivity of species within the nanoparticles[14]. Therefore, it is relevant to understand the structural changes taking place in the inner mesoporous structure when modified MSNs are in contact with biologically relevant environments. Dynamic light scattering (DLS) and transmission electron microscopy (TEM) provide information on changes in size and morphology of the MSNs triggered by buffer solutions, while nitrogen sorption allows tracing of variations in pore diameter along dissolution. However, from these techniques almost no information can be obtained on the inner structure and spatial organization of the mesoporous network.

Small Angle X-ray scattering (SAXS) provides information on the organization of the mesoporous structure and for this reason SAXS measurements have been extensively exploited in the past to finely characterize mesostructures and their growth mechanisms, taking advantage of synchrotron-

SAXS high flux and time resolution[15–17]. To our knowledge, no SAXS study has been yet reported that describes how MSN organization is affected by the exposure to pH and ionic conditions similar to those corresponding to human plasma. Ionic composition may be determinant in the degradation kinetics of MSNs, while silica dissolves and its concentration increases in media. For example, in the presence of metal ions such as $Ca^{2+}$ and $Mg^{2+}$, calcium/magnesium silicates precipitate at the silica surface, and prevent underlying silica from further dissolution. In addition, if the saturation concentration is eventually reached, silica can nucleate and re-precipitate on the MSN particles, hindering dissolution by depositing on the pores and decreasing the surface area[10,18,19]. In biological fluids the additional presence of proteins plays a fundamental role in the degradation as they absorb on the pores hampering pore dissolution. In this work we decided to focus on the degradation in the simulated body fluid (SBF) media without taking into account the presence of proteins for a better understanding of the phenomena faced by the MSNs in biological fluids, just addressing one variable of the dissolution process: the ionic conditions of the media. Furthermore, this step is essential before SAXS investigation on the dissolution of the MSNs in fully biological relevant conditions, because the SAXS signal from the protein will difficult -the experimental framework.

The aim of this work is to study by SAXS the protective effect of the PEG surface coating on the degradation of MSNs at physiological pH (7.4), and temperature (37 °C) in SBF. By means of SAXS it is possible to gain insight into the interplay between changes in particle morphology and mesopore arrangement. Dissolution experiments were conducted in a SBF solution, with ion concentrations close to those of human plasma. Exposure of MSNs to SBF resembles the ionic conditions that the nanoparticles could face during circulation in the human body. For this study we have chosen MSNs with MCM-48 pore structure (CTAB-templated, cubic pore arrangement

indexed in the space group *Ia3d*)[20], and monodisperse sizes below 200 nm in diameter, which are considered optimal for drug delivery. We performed experiments on naked (unmodified) and PEGylated MSNs.

We have worked with nanoparticle concentrations below, at and over the saturation concentration of silica in water, which is around 0.14 mg/mL at physiological temperature[21]. SAXS measurements performed at different time points during exposure revealed different structural changes of the MSNs in SBF solutions depending both on the MSN concentration, and on the presence of the PEG coating. Our results show how the MSN modification with PEG 5000 limits pore availability for the solvent and delays pore degradation, which is a fundamental aspect to be considered in the design of MSN carriers for drug delivery.

**Experimental section**

**Synthesis of Mesoporous Silica Nanoparticles (MSNs) MCM-48:** MSNs were synthesized following a method previously developed by Kim et al.[22] with minor modifications. First, 0.50 g of Hexadecyltrimethylammonium bromide CTAB (1.4 mmol) and 2.05 g of Pluronics F-127 (163 µmol) were dissolved in a solution formed by 96 mL of MilliQ water, 43 mL of ethanol (0.93 mol) and 11.2 mL of $NH_4OH$ 29% (180 mmol) under magnetic stirring at 1000 RPM for 30 minutes at room temperature, until complete dissolution. Then, 1.95 mL of Tetraethyl Orthosilicate, TEOS, (8.5 mmol) was added to the vortex of the solution under stirring at 1000 RPM. Stirring was continued for 1 additional minute to start the nucleation phase, then the sample left at room temperature under static conditions for 24 h to favor the process of nanoparticle growth and silica consolidation. A white solid was recovered from the solution and washed through centrifugations at room temperature. CTAB was extracted through acidic hydrolysis, under reflux conditions for 16 h in a mixture of 20 mL ethanol and 4 mL HCl 35%. MSNs were then washed and recovered

at 9000 RPM, and left to dry for 72 h at 60 °C for storage and subsequent functionalization. The extraction of surfactant was confirmed through FTIR spectroscopy. The size of the nanoparticles was determined by DLS and TEM, obtaining on average diameters of 178 nm, with PdI: 0.036 , and 140 ± 16 nm, respectively.(Figure S1)

**APTES functionalization:** All MSN prepared in this work were first modified with APTES, before PEGylation. Non PEGylated MSNs are always APTES modified. First, 10 µL APTES (0.1% in ethanol) was added to an MSN dispersion (1 mg/mL) in dry ethanol. The reaction was left stirring for 4 h at room temperature under inert atmosphere. Functionalized MSNs (MSN-$NH_2$) were washed and recovered at 9000 RPM. Grafting of APTES onto the MSN surface was demonstrated by FTIR (Figure S3) and changes in the z-potential(Table S1).

**PEG grafting**: 250 µg NHS-PEG(5kDa)-OH per 1 mg of MSN-$NH_2$ was added in 1 mL PBS 10 mM, pH 7.4. The reaction was left stirring for 2 h at room temperature. Subsequently, nanoparticles were washed three times with MilliQ water and recovered by centrifugation. The presence of PEG was confirmed by FTIR and TGA measurements. (Figure S3 and S4 respectively ) TGA was used to estimate density of PEG chains. After APTES and PEG functionalization, the thermogravimetric measurement shows a total organic content of 5% and 8%, respectively.

**Thermogravimetric analysis (TGA):** Using a TGA Discovery (TA instruments), thermogravimetric analysis were carried out in air at a flow rate of 25 mL/min. The samples were heated between 100 and 800°C at a rate of 10 °C per minute after being equilibrated at 100 °C for 20 min.

**Nitrogen adsorption – desorption isotherms:** Isotherms were recorded at 77 K using an Autosorb iQ3 Quantachrome equipment. Samples were degassed at 100°C for 12h prior to measurements. The Brunauer–Emmett–Teller (BET) equation was used to calculate the apparent surface area (SBET) from adsorption data obtained at P/P0. The pore size distribution was obtained using the Barret-Joyner-Halenda (BJH) model from the adsorption branch of the isotherm. The total pore volume (VTP) was obtained at P/P0 = 0.985. The micropore volume (Vμp) was calculated by means of α-plot method, using the LiChrospher Si-1000 macroporous silica gel as the reference adsorbent.

**SAXS**: SAXS experiments were performed at the Austrian beamline at the Elettra Synchrotron, Trieste, Italy. Measurements were carried out at 20 °C on an autosampler developed in the Austrian line, the μ-Drop sample changer, which provides a system for high-throughput automated microliter measurements of samples[23]. The μ-Drop system is configured to measure only a 15 μL drop in a capillary with a 1.5 mm OD / 0.01 mm borosilicate wall thickness (Hilgenberg, Maisfeld, Germany), encapsulated within a thermostatic compartment, connected to an external circulation bath and a thermal probe for temperature control. Incident and transmitted beam intensities were measured. Data for the transmission of the sample and the fluctuations of the primary beam were corrected, the scattering patterns of all the images of each sample were averaged and the respective backgrounds, treated in the same way, were subtracted. A Pilatus3 1M detector system recorded the two-dimensional patterns, processed by SAXS DOG[24] and by Igor Pro software (WaveMetrics, Lake Oswego, OR, USA) to obtain radial averages, hence the scattering intensity as a function of the magnitude of the scattering vector Q defined as $Q = 4\pi \sin\theta / \lambda$, with $2\theta$ being the scattering angle and $\lambda$ equal to 0.154 nm the wavelength of X-rays corresponding to an energy of 8 keV.

At least three different volumes of the same sample were measured at least four times for each volume, with an acquisition time of 10 s and a dwell time of 3 s for each step, hence an average of twelve acquisitions per sample was obtained. Both the MSN suspensions at concentration 1 mg/mL and the SBF were measured under the same conditions regarding temperature and exposure time. All the investigated conditions concern MSN suspensions at 1 mg/ml because lower concentrations did not result in a satisfactory SAXS signal.

**MSN degradation studies:** all the degradation tests were carried out for two systems in parallel, one corresponding to the MSN modified with APTES, and the other to the MSN covered with a 5 kDa PEG layer (hereinafter, MSN-$PEG_{5000}$).

To carry out the study of degradation, MSNs were exposed to simulated body fluid (SBF). This solution, proposed in the 1990s by Kokubo et al.[25], contains mineral ions in concentrations practically equal to those of human blood plasma, and has been recently proven to simulate the in vivo bone bioactivity of a material[26]. All dissolution tests were carried out in an incubator with horizontal shaking at 500 RPM at 37 °C to mimic physiological ionic conditions.

To compare the effects of dissolution on the particle morphology and mesopore arrangements, SAXS measurements were performed on APTES-modified MSN and MSN-$PEG_{5000}$ samples. Aging experiments were carried out in systems presenting concentrations i) below silica saturation at a concentration of 0.01 mg/mL, close to that used in animal experiments[3]; ii) at the saturation concentration of 0.14 mg/mL; and iii) well above saturation concentration at 1 mg/mL. Since MSN at concentration below 1 mg/mL resulted in a very low scattering signal although we used synchrotron radiation, large volumes of NPs in SBF solutions were prepared at the lowest concentrations of 0.01 and 0.14 mg/mL, and exposed to SBF for set time intervals. At defined time intervals, the solutions were centrifuged, MSN recovered, and the sample concentrated to 1 mg/mL.

Samples were then kept in ethanol until the measurements were performed, in order to avoid further degradation. For SAXS measurements, the medium was changed to SBF again, to maintain the same medium as in control experiments.

**TEM:** MSN nanoparticles were imaged in a JEOL JEM-1400PLUS LaB6-TEM (40kV – 120 kV, HC pole piece) equipped with a GATAN US1000 camera (2k x 2k).

**DLS**: Dynamic light scattering measurements were carried out with a Malvern Z-Sizer instrument in backscattering mode. All studies were performed at a 173° scattering angle, and temperature was kept at 25 °C in 1 mL polystyrene cuvettes.

**Results and discussion**

***a) Nanoparticle characterization.*** The synthesized MSN nanoparticles displayed the expected features of MCM-48. Figure 1 shows TEM micrographs of typical MSN nanoparticles, and a SAXS curve characteristic of organized mesoporous silica with well-defined diffraction peaks, which can be fitted as a cubic phase $Ia\bar{3}d$ with a unit cell size of $a$ = 8.7 nm. A surface area of 1058.8 $m^2\ g^{-1}$ and a monodisperse mesopore diameter of 2.7 nm were determined for the MSNs using nitrogen sorption measurements (Figure S5). DLS experiments showed a particle n averaged diameter of 178 nm as reported in (Figure S1).

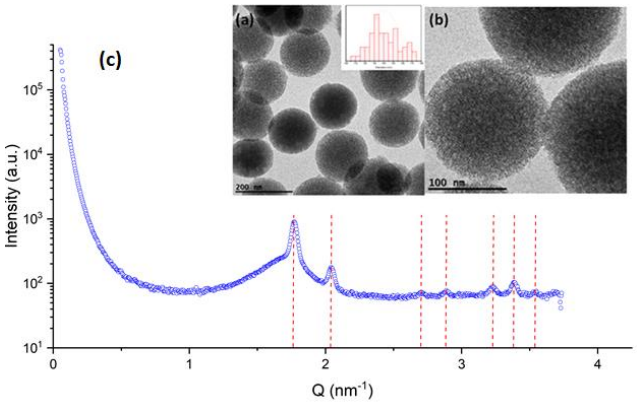


**Figure 1**. a) TEM micrograph of bare MSN particles. The inset shows a size distribution obtained from image analysis. b) Higher magnification image with a detailed observation of the mesopores. c) SAXS pattern of MSNs; the dashed lines indicate the diffraction peaks corresponding to the cubic phase 230. Diffraction peaks were analyzed with SCryPTA software.

PEG-functionalized MSNs present a distinctive core-shell structure. Analysis of TEM micrographs on ammonium molybdate-stained samples leads to *ca*. 110 nm silica cores surrounded by a *ca*. 15 nm less dense shell, attributable to the polymer (Figure 2a). TGA analysis (Figure S3) shows a PEG content of around 8.8% of total mass, leading to an estimation of a surface density of 1.5 PEG chains/nm$^2$. Nitrogen sorption measurements of amino-functionalized MSNs lead to a smaller surface area of 886 m$^2$ g$^{-1}$ while retaining mesopore size (Figure S5). After the PEG functionalization step, MSN surface was drastically diminished. Due to the very small sample quantity, the reproducibility was too low to show, but it can be assumed that the accessible surface area was below 100 m$^2$ g$^{-1}$, as previously reported[27].

SAXS profiles of MSNs-PEG$_{5000}$ show a noticeable change after PEG modification. Although the position of the main diffraction feature, typical of the regular internal pore array, remains in the same position after PEGylation, the peak becomes wider, and reflections corresponding to other

mesopore planes are lost. This effect can be due to partial pore blocking and/or to a certain interpenetration of PEG in the pores. This interpenetration could alter the apparent average distance between the pores, resulting in a less sharp peak, also leading to less intense scattering signals. We cannot completely rule out a possible degradation of the outer surface of the nanoparticles during the PEG grafting, that may cause a pore re-shaping due to local silica saturation and re-precipitation. Nevertheless, in the conditions of the functionalization with PEG (1 mg/mL in PBS at pH 7.4, 2h, r.t.), it seems unlikely that the degradation would be fast enough to lose the pore ordering to such a large extent. TEM images support this hypothesis as we can observe that pore ordering is retained after PEG functionalization (Figure 2b). Therefore, the PEG infiltration in the pores is in line with recent work by von Baeckmann et al, who found that the particular PEGylation method used here (i.e. MSN-$NH_2$ and NHS-PEG coupling) is accompanied with both a noticeable decrease in surface area and a loss of mesostructured organization, which suggest pore blocking during the functionalization process[27]. It is however worth noticing that these results cannot be simply generalized to any PEG functionalization, while they depend on the chemistry chosen for functionalizing the mesoporous nanoparticles with PEG and to the length and density of PEG chains themselves.

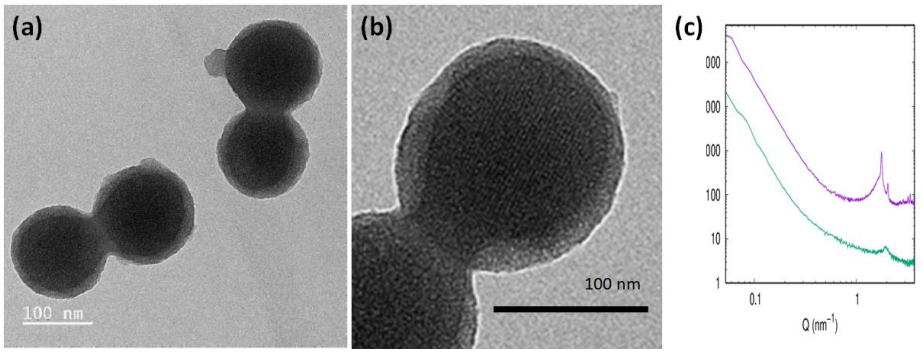


**Figure 2.** a) TEM micrograph of MSN-PEG$_{5000}$ particles. b) Detailed observation of the mesopores. c) Comparison between the SAXS patterns of MSNs-PEG (green) and MSNs (purple) at 1 mg mL$^{-1}$ concentration, before exposure of the nanoparticles to SBF.

***b) General evolution of MSN exposed to SBF.*** Dissolution experiments were carried out to establish general changes in morphology of PEGylated and non-PEGylated MSNs using electron microscopy combined with DLS. Concentrations were selected as above, within and below the silica solubility limits, 0.3, 0.14 and 0.02 mg/mL, respectively. MSNs were exposed to SBF for selected time intervals between 1 and 24 hours. DLS measurements performed in the aging solutions show an initial decrease in MSN diameter followed by aggregation (t > 6h) (data not shown); partial aggregation was observed visually. For silica concentrations near solubility (0.14 mg/mL), a fast aggregation of MSN is observed. These aggregation phenomena seem to take place, at least partially, at all concentrations preventing a proper estimation of the evolution of nanoparticle diameter. Therefore, DLS measurements were used only as a qualitative indication of size changes, while TEM measurements were used to obtain more detailed information on MSN degradation. Figure 3 shows representative TEM micrographs of MSNs and MSNs-PEG at 0.14 mg/mL silica concentration, i.e., near equilibrium exposed to SBF.

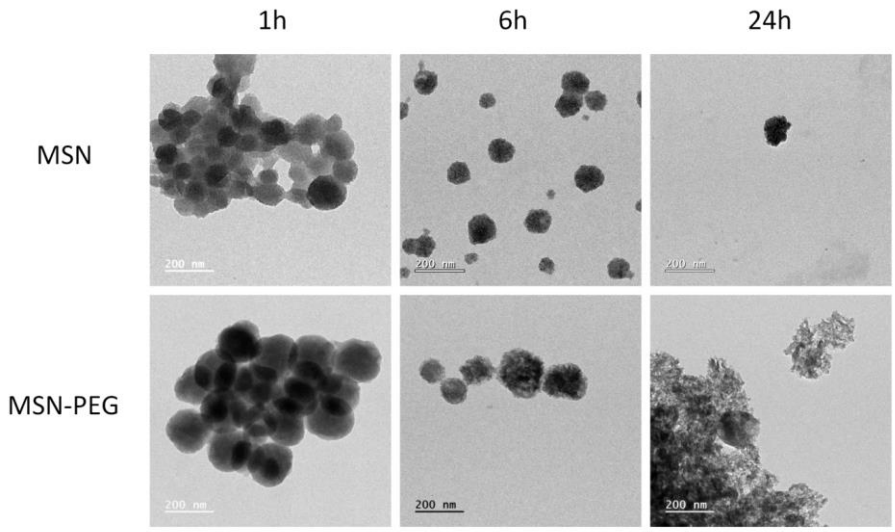


**Figure 3.** Representative TEM micrographs of MSN (above) and MSN-PEG (below) exposed to SBF for three time periods for a total silica concentration of 0.14 mg/mL.

Overall, a degradation of the mesoporous silica structure can be observed in all cases that leads to smaller, and aggregated nanoparticles. In some cases, a mesoporous structure is still clearly visible, even at long degradation times. Although some reprecipitation might take place, in most cases, a compact structure is conserved, instead of more complex morphological changes that can lead for example to hollow aggregates of smaller nanoparticles[5]. The variation in nanoparticle diameter for samples exposed for defined time periods to SBF, was determined by TEM (Figure 4). It is clear that dissolution is quite slow in the case of the more concentrated MSN solutions, in which a diameter ~~decrease~~decreases of ca. 20-25% is observed within 24 h. On the contrary, for lower concentrations, a fast decrease in diameter is observed in the case of bare MSN, leveling off at ca. 40 nm size in 24 h. In addition, PEGylated nanoparticles are significantly larger after exposure to SBF, indicating that PEG leads to stabilization from dissolution, even at low concentrations of silica. TEM results are in line with the general trends observed in the literature[8].

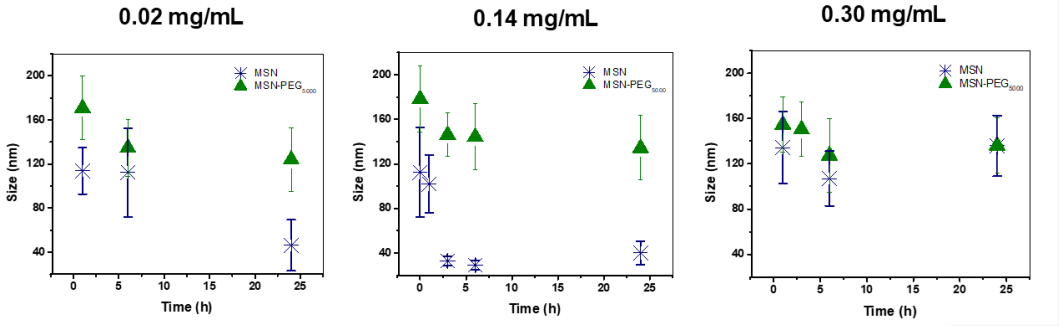


**Figure 4.** Variation of MSN diameter obtained from around 50-100 particles in TEM micrographs as a function of the time of exposure to SBF solutions for different total silica concentrations. MSN: blue symbols, MSN-PEG: green symbols.

***c) Detailed evolution of morphology and mesopore arrangement by SAXS.*** To shed light on the fate of the mesoporous structure, a SAXS study was performed. When non- PEGylated MSNs (i.e., only silanized with APTES ) were put in contact with the SBF solutions, a rapid loss of the SAXS diffraction peaks was observed after 30 minutes of incubation for the 0.01 and 0.14 mg/mL particle solutions (Figure S6). This is in agreement with the rapid decrease in diameter and morphological changes observed in the previous section. On the other hand, for MSN particles exposed to SBF at 1 mg/mL (Figure 5), a well-defined diffraction peak characteristic of organized mesopores is observed, which is detectable up to 24 h. Although the experimental noise does not allow a very reliable cell parameter to be calculated, the relationship between the distances of the more intense diffraction peaks located at approximately Q = 1.88 $nm^{-1}$ and Q = 2.16 $nm^{-1}$ can be attributable to peaks [211] and [220] of the cubic phase and permits estimation of a cubic cell constant of ca. $a$ = 8.2 nm. This value is substantially smaller than the original cell parameter of 8.7 nm (see Figure 1). We propose that in a first stage, there is a rapid dissolution process that causes a partial collapse of the mesoporous structure. It is known that the walls of CTAB-templated materials such as

MCM-48 are thin (~1 nm)[14], so even a small loss of material can lead to a significant decrease in the network parameter, as it has been found in MCM-48 exposed to media containing phosphate[10,28].

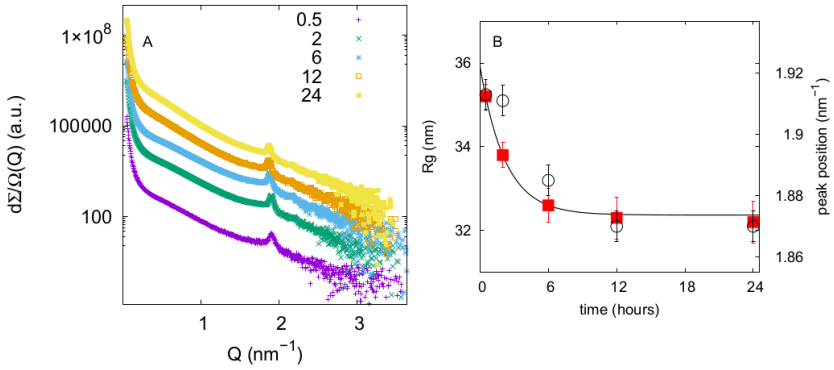


**Figure 5.** (a) SAXS patterns of bare MSNs suspended in SBF at 1 mg/mL at different time intervals of exposure, as reported in the legend in unit of hours. The diffraction peak is still maintained after 24 hours of degradation in SBF. SAXS curves are scaled for clarity. (b) Radii of gyration estimated from SAXS (red squares) and the position of the [211] X-ray diffraction peak of the cubic mesophase (empty circles) graphed as a function of incubation time in SBF. The solid line is the theoretical fit of the experimental points obtained by the exponential laws $R_G = R_0 e^{-t/\tau} + c$ and $Q_p = Q_{p_0} e^{-t/\tau} + d$, where c and d are bare constants, while τ is the time constant. $\tau = 2.2 \pm 0.2\ hours$, $R_0 = 36.1 \pm 0.9\ nm$, $Q_{p_0} = 1.874 \pm 0.005\ nm^{-1}$.

Along exposure to SBF solutions, a slight shift in the position of the diffraction peaks towards lower Q values is observed throughout the incubation time. This displacement implies a very small increase in the cell parameter during incubation from 8.1 to 8.3 nm. This result can be read considering the hypothesis, recently reviewed in (https://link.springer.com/content/pdf/10.1007/s10971-021-05695-8.pdf ), concerning the complete degradation in aqueous media of different silica nanoparticles based on their porosity and composition. The investigated MSN should reduce their pores size during aging. The

Formattato: Allineato a sinistra

Codice campo modificato

decrease of the position of the peak (Fig.s 5a ans 5b) during aging, and the consequent increase of cell parameters, is expected to be related to the increase of the wall thickness, as evidenced in (https://www.sciencedirect.com/science/article/pii/S1387181122003365). ~~which suggests that in a second stage, the degradation involves a slight but progressive increase in inter-pore distances within the internal structure of MSNs.~~ Therefore, we can propose that immersion of the MSN in SBF solution might induce a slight contraction due to the capillary forces developed under wetting.[29] Upon dissolution, the resulting strain is released, leading to a slow relaxation of the mesopore structure that is reflected in the observed increase in the ~~mesostructure~~ cell parameter. Note that because we have SAXS curves in solution, we cannot observe the whole pattern of X-ray diffraction peaks to determine not only the pore-to-pore distance, but also the pore diameter of the mesoporous materials, as recently performed and simulated (https://pubs.acs.org/doi/10.1021/jp4057362). Hence, we cannot assure that the density of water confined in the mesopore is similar to the bulk density, although there are several discussions about the abnormal physical properties of molecules confined within nanospaces. Also, we cannot determine if the pore form factor is changing during aging. Consequently, at the light of previous results, we believe that the little but appreciable change in cell parameter is related to pore size decrease and/or to water condensation into mesopores, partly due to the chemisorption of additional matter within the porous network (https://pubs.acs.org/doi/10.1021/la050981z). ~~However, i~~It is interesting to note ~~in this case,~~ that well above the silica solubility limit, the MSN mesostructure is conserved along 24 hours (Figure 5a).

On the other hand, the dispersion can be analyzed at low Q values (Guinier Region), which allows for calculating the radius of gyration ($R_G$), which is an estimator of the MSNs average size. The radius of gyration $R_G$ of a particle is defined as the mean square root of the distance of all electrons

from its center of gravity, in complete analogy with the radius of inertia in mechanics, with the only difference that here the electrons take the place of mass elements. Therefore, $R_G$ can be easily calculated for simple geometric bodies. Considering that our systems can be roughly modeled as a solid sphere of radius $r$, the radius of gyration $R_G$ determined by SAXS is: $R_G = \sqrt{\frac{3}{5}}r$. Hence, the radii $r$ of MSNs, obtained from the Guinier region analysis, range from about 41 to 46 nm, in agreement with the trend and size of diameters obtained by TEM (see Figure 4).

In SAXS curves (Figure 5a), a change in curvature is observed at low Q values over time, corresponding to a decrease in the average particle size (Figure 5b). If both the radii of gyration obtained in the Guinier approximation $R_G$, and the position of the diffraction peak $Q_p$ are plotted as a function of time, it can be observed that these two parameters show exactly the same dependence as a function of time, as seen by the theoretical fit (continuous black line in Figure 5b).

The time constant τ resulting from the simultaneous fit of both the gyration radius and the peak position behavior as a function of time of exposure to SBF, is equal to (2.2±0.2) h. This result

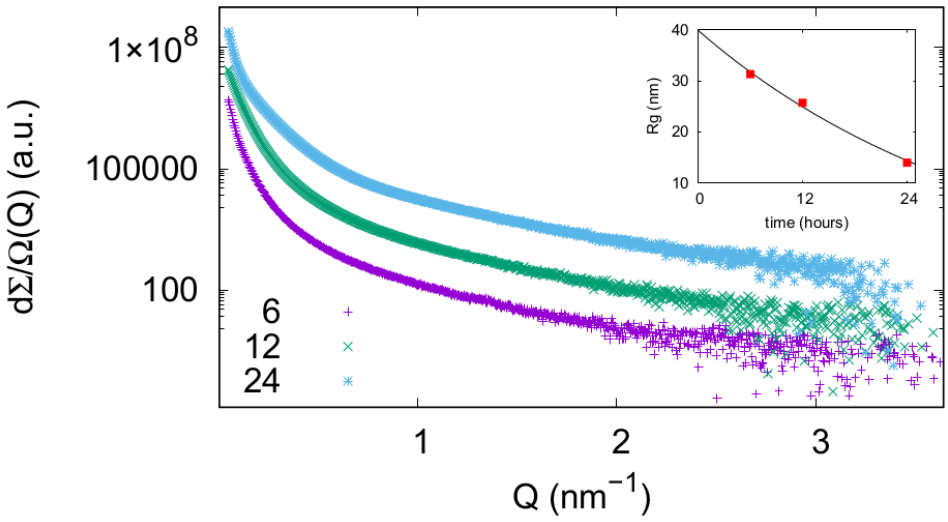


**Figure 6**. SAXS patterns of MSNs-PEG$_{5000}$ in SBF 0.01 mg/mL at different exposure times in SBF, as reported in the legend in units of hours. The presence of peaks corresponding to the mesoporous structure is not observed. SAXS curves are scaled for clarity. Inset: evolution of $R_G$ obtained from the Guinier region along time.

shows that the dissolution of MSNs and the ~~loss of order~~changes in the internal structure of mesoporous particles are interconnected phenomena that take place on the same time scale.

It could also be noted that MSNs at 1 mg/ml do not significantly evolve after 6 hours: both the radius of gyration and the position of the diffraction peak do not change as the silica continues to hydrolyze; it is possible that some reprecipitation of the amorphous silica occurs under these concentrated conditions, as already reported for MSNs in SBF[18]. The incorporation of material in the pores could also contribute to the slight "swelling" of the mesostructures observed. This could cause a partial reduction in the specific surface area involved in the dissolution.~~, which results in the pores not being further degraded.~~ We can speculate that, after 6 hours under the

conditions employed, the reprecipitation process has been effective in blocking pore access, and the hydrolysis-condensation equilibrium is reduced only to the outer surface of the MSNs.

Although in Figures 5 and 6 SAXS curves are scaled for the sake of clarity, it can be noticed an increase in the scattering intensity at Q≈0 as the degradation proceeds. A possible explanation for this could be the increase in aggregation of the sample with time and the appearance of smaller nanoparticles cleaved from the MSNs, which can be appreciated very well in the TEM images. The formation of aggregates would result in more scatter than single particles, although large aggregates would not be detected by SAXS. The increase in the number of scattering objects, with the appearance of small nanoparticles cleaved from the MSNs or produced by the precipitation of silica dissolved from the MSNs will also increase the scattering intensity. The increase in scattering intensity with time of exposure to the SBF can be as well appreciated in the rest of the samples.In the SAXS curves of MSNs-$PEG_{5000}$ at the lowest silica concentration of 0.01 mg/mL, a concentration comparable to that used for *in vivo* experiments[3], no characteristic peak of mesostructure can be seen (Figure 6). This result, as already observed for naked MSNs, implies that the ordered internal structure that comes from the arrangement of the pores is quickly lost, partially in the functionalization (as discussed above), and partially in the first dissolution stage, leading to wider, more irregular pores. This loss of organization of the mesopores is reflected in a rapid decrease in the diffraction signal at low angles. It can then be concluded that even in PEG-protected MSNs, the morphological rearrangement of silica already observed by TEM is reflected in the destruction of organized mesoporosity in these diluted systems, from the very initial stages of dissolution. From the analysis of the SAXS curves at low Q values, in the Guinier region, the gyration radius of the MSNs displays again a progressive decrease (Figure 6, inset), consistent with the TEM images (not shown).

For more concentrated MSNs-PEG$_{5000}$, near equilibrium (silica concentration of 0.14 mg/mL), a small peak located at Q = 1.61 nm$^{-1}$ can be observed within the first 30 minutes of incubation in SBF, which disappears after 2 h (Figure 7). The presence of a single diffraction peak corresponding to a larger cell with a low intensity is indicative of a more disordered structure, and suggests that rapid degradation occurs, modifying the order of the mesopores. However, it is clear that this degradation is slower for MSNs decorated with PEG than for naked MSNs.

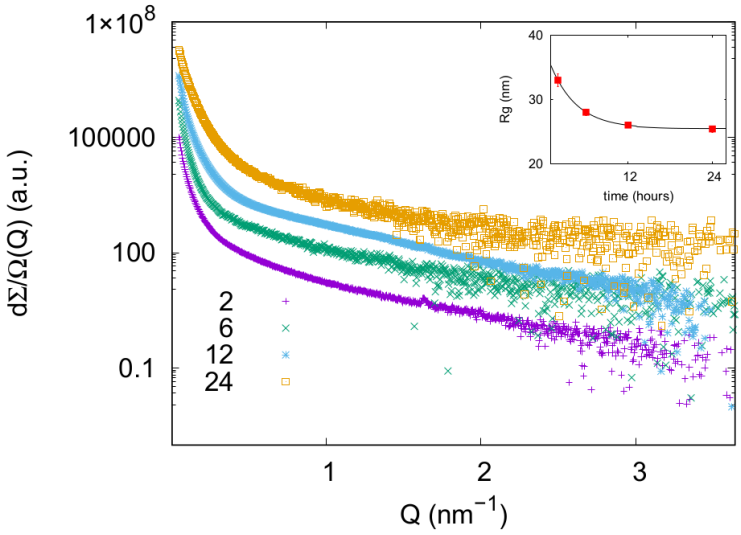


**Figure 7.** SAXS curves of MSNs-PEG at 0.14 mg/mL in SBF at different degradation times, as reported in the legend in units of hours. SAXS curves are scaled for clarity.. In the inset, gyration radii fitted with a τ=(3.7±0.2) hours.

The inset in Figure 7 shows the radii of gyration $R_G$ obtained by Guinier's approximation for the low Q values, as a function of the degradation times for the MSNs-PEG$_{5000}$ at the saturation concentration. $R_G$ evolution as a function of time is qualitatively similar to that found without PEG (see Figure 5b), but slower, since in this latter case the parameter τ is higher: 3.7 h for MSNs-PEG, and 2.2 h for naked MSNs. This point confirms the effectiveness of PEG toward MSN degradation. It must be stressed that even if we are close to the saturation of silica in these conditions, at a

concentration of particles of 0.14 mg/mL we are still below the saturation limit, as 0.14 mg/mL is the maximum concentration of dissolved silica, and to be reached, a consistent part of the particles need to dissolve, as we see from SAXS curves and TEM images.

In SAXS patterns obtained for MSNs-PEG at 1 mg/mL the diffraction peak does not change its position after 24 hours of incubation in SBF, therefore no noticeable degradation is observed (Figure 8). This result is as expected for such a high concentration of MSNs, well above silica solubility limit. TEM and SAXS results confirm that PEGylation has a protective effect on the structure of mesoporous nanoparticles and on the arrangement of their pores. The PEGylation process leads to a less well-defined SAXS mesopore signal, probably because the PEG chains occupy part of the pores, thereby blurring the contrast in electron density. In principle, this effect could be due to the silanization and the following PEGylation possibly taking place also on the pore walls, as the polymer is capable of diffusing along the mesopores due to its relatively low molecular weight of 5 kDa. The change of peak positions in SAXS curves during aging evidenced in Figure 5 has to be compared to the steady peaks reported in Figure 8, concerning the same sample concentration and different PEGylation.

In fact ~~A~~after PEGylation, the order of the pores is maintained at 1 mg/mL of MSNs-PEG, without observing any appreciable change in the arrangement of the peaks with time, up to 24 h of exposure. ~~, O~~only a slight reduction in particle size is observed. This result is not surprising, because previous studies reported that colloidal mesoporous silica PEGylated particles still show the original mesoporous structure after 1 month immersion in SBF at 37 °C (see Figure 10 in https://www.sciencedirect.com/science/article/pii/S1387181109005216?via%3Dihub ). The lack of changes in peak position in Figure 8 evidence that the presence of a PEGylated surface inhibits water penetration into MSN and internal structure modifications.

TEM images of these MSNs show well-defined mesopores, although some aggregation takes place (data not shown).

On the contrary, even at high concentrations (0.3-1 mg/mL), the absence of PEG induces significant changes in the mesopore arrangement, as demonstrated by the morphological changes observed by TEM, and the progressively longer interpore distances. These changes take place mostly in the first hours of exposure and are a consequence of the dynamic dissolution-reprecipitation of silica in the porous network due to the SBF environment. No major changes in pore size and organization can be seen after 6 hours, when it is possible that the decrease in the porous surface could block the solution, slowing down the degradation.

At lower silica concentrations near equilibrium (0.14 mg/mL), the protective effect of PEG is significant, although morphological changes still take place due to the fast degradation kinetics.

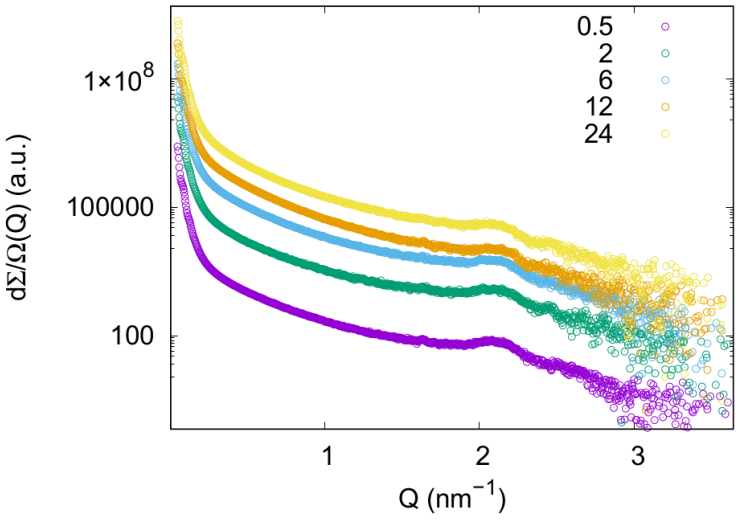


**Figure 8**. MSNs-$PEG_{5000}$ in SBF at 1 mg/ml, the legend provides the aging in term of hours. The diffraction peak remains at the same position for all exposure times. SAXS curves are scaled for clarity.

After 30 minutes of degradation in SBF, an ordered porous network is still present within the MSNs-PEG, reflected in a diffraction peak that disappears after 2 h of degradation. This means that the order of the pores is lost during degradation, following a dissolution pattern from the interior of the particle, as already reported for some MSN structures[13], or, more likely, dissolving both from the interior and from the outer surface simultaneously, as observed by Kuroda et al.[30] This last hypothesis seems to be the most appropriate, since the dispersion at low Q values points to a continuous decrease in the size of MSN during the 24 h of the study, which shows that the outer surface of the particles is also dissolving, reducing the particle size. Since the silica concentration is close to saturation, the dissolution of the silica can proceed in a dynamic equilibrium where the MSNs dissolve and the silica re-precipitates over time, causing the aggregation of particles, as observed in the TEM images (Figure 3).

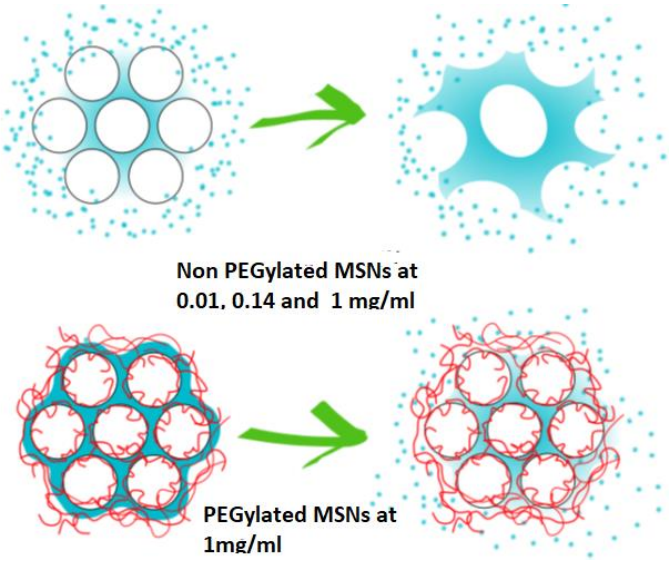

**Figure 9** Scheme showing the protective effect of PEGylation on the dissolution of MSNs in SBF at neutral pH. Non PEGylated MSNs loose their structural features as sketched by the changes in pore and wall characteristics while PEGylated MSNs retain their structural features, which is sketched by not showing changes in the pores and walls of the MSN after exposure to SBF.

## Conclusions

SAXS studies show distinct differences in organization of MSNs and MSNs-$PEG_{5000}$ with the time of exposure to SBF, with a strong concentration dependence.

The rapid degradation, reprecipitation and aggregation of MSNs below and near the saturation concentration of silica observed by TEM correlates with a rapid loss of order in the porous structure, suggesting a dissolution mechanism involving the inner core of the particles.

At a higher concentration, above the saturation concentration of silica, the order of the pores is retained during dissolution. A good time correlation is observed between changes in interpore distances and the decrease in particle size for non-PEGylated MSNs, both taking place within 6 hours. It is assumed that within this time, reprecipitation and saturation of the solution has taken place.

It can be concluded that PEG has a clear protective effect on the pore structure, slowing down the degradation as seen in all samples with a silica concentration above 0.14 mg/mL, which suggests that the polymer acts as a protective barrier, avoiding hydrolysis and release of silicate species, and aiding to maintain relatively high local concentrations of silica that kinetically hinder massive dissolution. The protective effect of PEG in preventing degradation results in the retention of structural features by PEGylated MSN while these are lost in the non-PEGylated ones. This effect has been sketched in Figure 9. Overall, our results highlight the fragility of these mesostructures under conditions similar to those found in vivo of pH and ionic composition and strength. They further underscore the importance of coating the external surface with polymers to extend the

degradation time of the particles, necessary for a controlled delivery of active principles or drugs. On the other hand, our work reveals the complexity of the dissolution processes of these materials, and the transformations that take place above silica saturation.

**Acknowledgements**

The authors thank Elettra Synchrotron for beamtime allocation and acknowledge the CERIC-ERIC Consortium for the access (20192044 proposal code) to experimental facilities. S.E.M. thanks the PID2020-114356RB-I00 project from the Ministry of Science and Innovation of the Government of Spain. G.S.I. acknowledges support from ANPCyT (PICT 2015–2526 and PICT 2018–4651). This work was performed under the Maria de Maeztu Units of Excellence Program from the Spanish State Research Agency - Grant no. MDM-2017-0720. PA gratefully acknowledge the financial support of Consorzio Sistemi a Grande Interfase (C.S.G.I.). We acknowledge Julia Cope, PhD from CIC biomaGUNE for kindly revising the manuscript.

**References:**

[1] M. Vallet-Regí, M. Colilla, I. Izquierdo-Barba, M. Manzano, Mesoporous Silica Nanoparticles for Drug Delivery: Current Insights, Molecules. 23 (2017) E47.
[2] J. Lu, M. Liong, Z. Li, J.I. Zink, F. Tamanoi, Biocompatibility, Biodistribution, and Drug-Delivery Efficiency of Mesoporous Silica Nanoparticles for Cancer Therapy in Animals, Small. 6 (2010) 1794–1805.
[3] E. Bindini, M. de los A. Ramirez, X. Rios, U. Cossío, C. Simó, V. Gomez-Vallejo, G. Soler-Illia, J. Llop, S.E. Moya, In Vivo Tracking of the Degradation of Mesoporous Silica through 89Zr Radio-Labeled Core–Shell Nanoparticles, Small. 17 (2021) 2101519.
[4] Y. Wang, Q. Zhao, N. Han, L. Bai, J. Li, J. Liu, E. Che, L. Hu, Q. Zhang, T. Jiang, S. Wang, Mesoporous silica nanoparticles in drug delivery and biomedical applications, Nanomedicine: Nanotechnology, Biology and Medicine. 11 (2015) 313–327.
[5] C.-Y. Lin, C.-M. Yang, M. Lindén, Dissolution and morphology evolution of mesoporous silica nanoparticles under biologically relevant conditions, Journal of Colloid and Interface Science. 608 (2022) 995–1004.

[6] T. L. Nguyen,Y.Choi,J. Kim Mesoporous Silica as a Versatile Platform for Cancer Immunotherapy Advanced Materials 23 (2019) 1803953.

[7] Y. Hu, S. Bai, X. Wu, S. Tan, Y. He, Biodegradability of mesoporous silica nanoparticles, Ceramics International. 47 (2021) 31031–31041.
[8] V. Cauda, C. Argyo, T. Bein, Impact of different PEGylation patterns on the long-term bio-stability of colloidal mesoporous silica nanoparticles, J. Mater. Chem. 20 (2010) 8693.
[9] Y.S. Lin, N. Abadeer, C.L. Haynes, Ultrastable and redispersible mesoporous silica nanoparticles for targeted anticancer drug delivery: Materials Engineering and Sciences Division - Core Programming Topic at the 2011 AIChE Annual Meeting, Materials Engineering and Sciences Division - Core Programming Topic at the 2011 AIChE Annual Meeting. (2011) 914–915.
[10] V. Cauda, A. Schlossbauer, T. Bein, Bio-degradation study of colloidal mesoporous silica nanoparticles: Effect of surface functionalization with organo-silanes and poly(ethylene glycol), Microporous and Mesoporous Materials. 132 (2010) 60–71.
[11] K.S. Butler, P.N. Durfee, C. Theron, C.E. Ashley, E.C. Carnes, C.J. Brinker, Protocells: Modular Mesoporous Silica Nanoparticle-Supported Lipid Bilayers for Drug Delivery, Small. 12 (2016) 2173–2185.
[12] C. Argyo, V. Weiss, C. Bräuchle, T. Bein, Multifunctional Mesoporous Silica Nanoparticles as a Universal Platform for Drug Delivery, Chem. Mater. 26 (2014) 435–451.
[13] T. Tanaka, B. Godin, R. Bhavane, R. Nieves-Alicea, J. Gu, X. Liu, C. Chiappini, J.R. Fakhoury, S. Amra, A. Ewing, Q. Li, I.J. Fidler, M. Ferrari, In vivo evaluation of safety of nanoporous silicon carriers following single and multiple dose intravenous administrations in mice, International Journal of Pharmaceutics. 402 (2010) 190–197.
[14] K. Braun, A. Pochert, M. Beck, R. Fiedler, J. Gruber, M. Lindén, Dissolution kinetics of mesoporous silica nanoparticles in different simulated body fluids, J Sol-Gel Sci Technol. 79 (2016) 319–327.
[15] D. Grosso, A.R. Balkenende, P.A. Albouy, A. Ayral, H. Amenitsch, F. Babonneau, Two-Dimensional Hexagonal Mesoporous Silica Thin Films Prepared from Block Copolymers: Detailed Characterization and Formation Mechanism, Chem. Mater. 13 (2001) 1848–1856.
[16] C. Boissiere, D. Grosso, H. Amenitsch, A. Gibaud, A. Coupé, N. Baccile, C. Sanchez, First in-situ SAXS studies of the mesostructuration of spherical silica and titania particles during spray-drying process, Chem. Commun. (2003) 2798–2799.
[17] Tuning of the Temperature Window for Unit-Cell and Pore-Size Enlargement in Face-Centered-Cubic Large-Mesopore Silicas Templated by Swollen Block Copolymer Micelles - Li - 2015 - Chemistry – A European Journal - Wiley Online Library, (n.d.).
[18] R. Mortera, S. Fiorilli, E. Garrone, E. Verné, B. Onida, Pores occlusion in MCM-41 spheres immersed in SBF and the effect on ibuprofen delivery kinetics: A quantitative model, Chemical Engineering Journal. 156 (2010) 184–192.
[19] T. Fontecave, C. Sanchez, T. Azaïs, C. Boissière, Chemical Modification As a Versatile Tool for Tuning Stability of Silica Based Mesoporous Carriers in Biologically Relevant Conditions, Chem. Mater. 24 (2012) 4326–4336.
[20] K. Schumacher, P.I. Ravikovitch, A. Du Chesne, A.V. Neimark, K.K. Unger, Characterization of MCM-48 Materials, Langmuir. 16 (2000) 4648–4654.
[21] R.O. Fournier, J.J. Rowe, The solubility of amorphous silica in water at high temperatures and high pressures, American Mineralogist. 62 (1977) 1052–1056.

[22] T.-W. Kim, P.-W. Chung, Facile Synthesis of Monodispersed MCM-48 Mesoporous Silica Nanoparticles with Controlled Particle Size, (n.d.) 14.
[23] R. Haider, B. Sartori, A. Radeticchio, M. Wolf, S. Dal Zilio, B. Marmiroli, H. Amenitsch, µDrop: a system for high-throughput small-angle X-ray scattering measurements of microlitre samples, J Appl Crystallogr. 54 (2021) 132–141.
[24] M. Burian, B. Marmiroli, A. Radeticchio, C. Morello, D. Naumenko, G. Biasiol, H. Amenitsch, Picosecond pump–probe X-ray scattering at the Elettra SAXS beamline, J Synchrotron Rad. 27 (2020) 51–59.
[25] T. Kokubo, H. Kushitani, S. Sakka, T. Kitsugi, T. Yamamuro, Solutions able to reproduce in vivo surface-structure changes in bioactive glass-ceramic A-W3, Journal of Biomedical Materials Research. 24 (1990) 721–734.
[26] T. Kokubo, H. Takadama, How useful is SBF in predicting in vivo bone bioactivity?, Biomaterials. 27 (2006) 2907–2915.
[27] C. von Baeckmann, G.M.D.M. Rubio, H. Kählig, D. Kurzbach, M.R. Reithofer, F. Kleitz, Evaporation-Induced Self-Assembly of Small Peptide-Conjugated Silica Nanoparticles, Angewandte Chemie International Edition. 60 (2021) 22700–22705.
[28] E. Bindini, Z. Chehadi, M. Faustini, P.-A. Albouy, D. Grosso, A. Cattoni, C. Chanéac, O. Azzaroni, C. Sanchez, C. Boissière, Following in Situ the Degradation of Mesoporous Silica in Biorelevant Conditions: At Last, a Good Comprehension of the Structure Influence, ACS Appl. Mater. Interfaces. 12 (2020) 13598–13612.
[29] G. Dolino, D. Bellet, C. Faivre, Adsorption strains in porous silicon, Phys. Rev. B. 54 (1996) 17919–17929.
[30] H. Yamada, C. Urata, Y. Aoyama, S. Osada, Y. Yamauchi, K. Kuroda, Preparation of Colloidal Mesoporous Silica Nanoparticles with Different Diameters and Their Unique Degradation Behavior in Static Aqueous Systems, Chem. Mater. 24 (2012) 1462–1471.